Available online at www.sciencedirect.com
SCIENCE DIRECT®
Journal of Microbiological Methods 59 (2004) 395–413
Journal of Microbiological Methods
www.elsevier.com/locate/jmicmeth

Three-dimensional biofilm structure quantification

Haluk Beyenal[a], Conrad Donovan[a], Zbigniew Lewandowski[a,b,*], Gary Harkin[c]

[a]Center for Biofilm Engineering, P.O. Box 173980, Room 366 EPS, Montana State University, Bozeman, MT 59717-3980, United States
[b]Department of Civil Engineering, Montana State University, Bozeman, MT 59717, United States
[c]Computer Science Department, Montana State University, Bozeman, MT 59717, United States

Received 29 March 2004; received in revised form 16 August 2004; accepted 17 August 2004
Available online 23 September 2004

Abstract

Quantitative parameters describing biofilm physical structure have been extracted from three-dimensional confocal laser scanning microscopy images and used to compare biofilm structures, monitor biofilm development, and quantify environmental factors affecting biofilm structure. Researchers have previously used biovolume, volume to surface ratio, roughness coefficient, and mean and maximum thicknesses to compare biofilm structures. The selection of these parameters is dependent on the availability of software to perform calculations. We believe it is necessary to develop more comprehensive parameters to describe heterogeneous biofilm morphology in three dimensions.

This research presents parameters describing three-dimensional biofilm heterogeneity, size, and morphology of biomass calculated from confocal laser scanning microscopy images. This study extends previous work which extracted quantitative parameters regarding morphological features from two-dimensional biofilm images to three-dimensional biofilm images. We describe two types of parameters: (1) textural parameters showing microscale heterogeneity of biofilms and (2) volumetric parameters describing size and morphology of biomass. The three-dimensional features presented are average (ADD) and maximum diffusion distances (MDD), fractal dimension, average run lengths (in X, Y and Z directions), aspect ratio, textural entropy, energy and homogeneity. We discuss the meaning of each parameter and present the calculations in detail. The developed algorithms, including automatic thresholding, are implemented in software as MATLAB programs which will be available at www.erc.montana.edu site prior to publication of the paper.

Keywords: Biofilm; Structure; 3-Dimension; Quantification; Modeling; Image; ISA3D

1. Introduction

Three-dimensional image analysis has been used to quantify limited numbers of parameters calculated from confocal scanning laser microscopy images (CSLM). Initial efforts at quantifying structure from CSLM images came from Kuehn

* Corresponding author. Tel.: +1 406 994 5915; fax: +1 406 994 6098.
E-mail address: ZL@erc.montana.edu (Z. Lewandowski).

0167-7012/$ - see front matter © 2004 Elsevier B.V. All rights reserved.
doi:10.1016/j.mimet.2004.08.003

et al. (1998), who calculated biovolume of biofilms (Kuehn et al., 1998). Heydorn et al. (2000) developed a software package (COMSTAT) to calculate biovolume, surface area coverage in each layer, biofilm thickness distribution, average biofilm thickness, volumes of micro-colonies identified at the substratum, the fractal dimension of each microcolony identified at the substratum, roughness coefficient, distributions of diffusion distance and maximum diffusion distance, and surface to volume ratio from a three-dimensional stack of biofilm images (Heydorn et al., 2000). This work suggested the use of the mean thickness as an important parameter for describing biofilm structure and in the following paper (Heydorn et al., 2002) they used the mean thickness and the roughness coefficient to describe biofilm structure. Following their recommendations many authors used the mean and maximum thicknesses and the roughness coefficient to describe biofilm structure and as the criteria for their conclusions when they compared biofilm structures (Battin et al., 2003; Christensen et al., 2002; Hentzer et al., 2001; Hinsa et al., 2003; Kierek and Watnick, 2003; Mah et al., 2003; Martiny et al., 2003). As an alternative to COMSTAT, Xavier et al. (2003) developed software to quantify biovolume, substratum coverage, average height of microcolonies, and interfacial area. This software had the advantage of automatically thresholding images, but only provided four parameters. We believe most of the literature studies presented above used average thickness, roughness coefficient, and biovolume to describe biofilm structure because additional three-dimensional analytical parameters were not available in the literature.

A parameter describing biofilm morphology in three dimensions must be calculated from the variation of pixel intensities in three-dimensional image sets. Formerly described parameters, such as roughness coefficient and average biofilm thickness (Heydorn et al., 2000) are one-dimensional, providing information only in the direction perpendicular to the biofilm surface. Biovolume and surface to volume ratio are related to magnitude of biomass in the biofilm and were not calculated using pixel intensity variations in three dimensions. The parameters described by Heydorn et al. (2000) and Xavier et al. (2003) could be improved to describe three-dimensional heterogeneous biofilm morphology more comprehensively. In addition, the parameters calculated by Heydorn et al. (2000) using COMSTAT require manual thresholding, which can introduce significant errors in biofilm image analysis and can lead to completely different conclusions (Beyenal et al., 2004; Xavier et al., 2001; Yang et al., 2001). The implementation of automatic thresholding during the calculations of morphological parameters would produce more robust results.

The goal of this study is to further develop the previous software of COMSTAT, Xavier et al. (2003) and ourselves (ISA) (Beyenal et al., 2004; Yang et al., 2000) by describing more comprehensive parameters in three dimensions. This paper describes the calculation of average and maximum diffusion distances, fractal dimension, average run lengths (in X, Y and Z directions), aspect ratio, textural entropy, energy, and homogeneity from three-dimensional images acquired by CSLM. We illustrate the calculation of each parameter and provide simple examples to help researchers understand their meanings. The described algorithms, including automatic thresholding as described by (Beyenal et al., 2004; Yang et al., 2000), are integrated in software named Image Structure Analyzer in 3 Dimensions, ISA3D, which will be available at www.erc.montana.edu prior to publication of this paper.

2. Quantifying structural parameters

2.1. Layered concept of CSLM images

Fig. 1A shows the coordinate system used in this paper. The CSLM images are acquired in layers parallel to the biofilm surface. Each layer corresponds to an image in the X and Y directions and the layers are treated as the Z direction. The schematic diagram of a single layer is presented in Fig. 1B, where each pixel is represented as an (x, y, z) triplet, and dx and dy are defined as the size of a pixel in the X and Y directions. For all CSLM images, dx=dy

and, for our example, let us assume that dx=dy=1 μm in Fig. 1B.

An additional layer shown in Fig. 1C introduces dz', the distance between layers in the image set. Because of computer memory limitations, users typically acquire CSLM images with dz' greater than dx or dy. Having dx=dy≠dz' biases the calculation of some three-dimensional parameters. To avoid this problem, additional layers are calculated by interpolation so that the pixel size is the same in all three directions, dx=dy=dz (Fig. 1D).

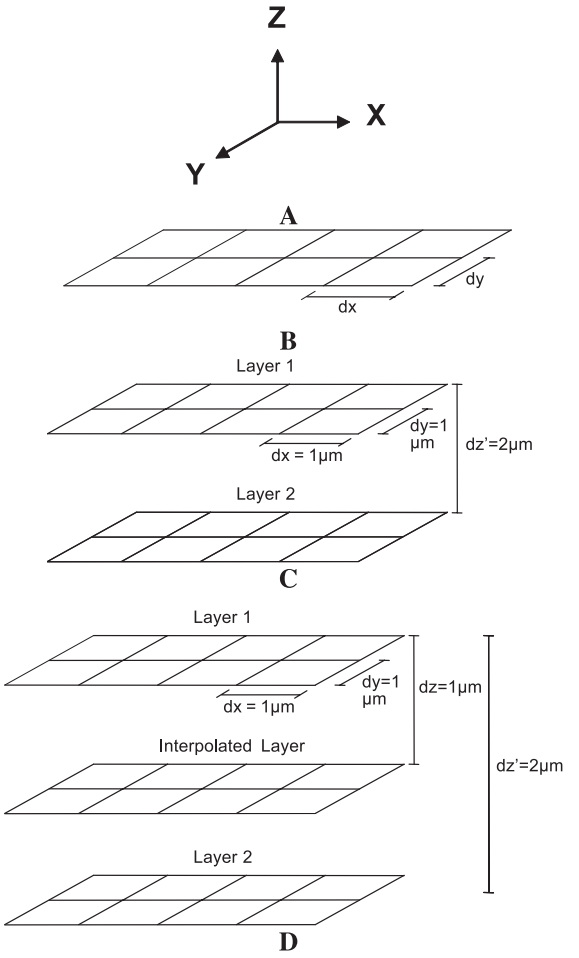

Fig. 1. (A) coordinate system used in the manuscript, (B) single layer of image, (C) image with two layers with a distance between layers of dz'=2 μm, (D) layers 1, layer 2 and the interpolated layer; dx=dy=dz=1 μm.

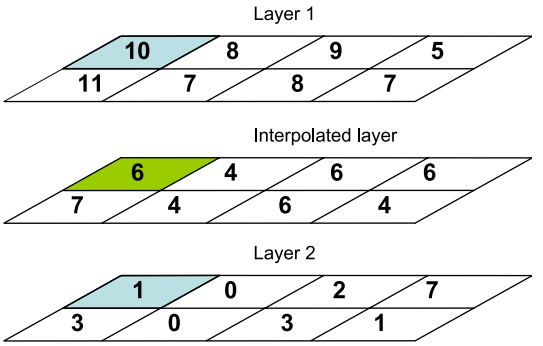

Fig. 2. Linear method of interpolation. CSLM images for layers 1 and 2 were acquired. We generated the interpolated layer to make dx=dy=dz and produce more accurate results.

2.2. Interpolation of three-dimensional biofilm images

A simple method of interpolation is the "linear" method, which looks at the same cell coordinates in successive layers to calculate the average pixel values to form the interpolated layer. For example, in Fig. 2, the values of pixels at locations layer 1 (1,1) and layer 2 (1,1) are 10 and 1, respectively. The interpolated image at (1,1) is 6 since (10+1)/2=5.5 and 5.5 is rounded to the nearest integer, 6, because pixel values must be integers. The other (x,y) coordinates for interpolated layers are calculated in the same manner.

We used linear interpolation due to its simplicity, but there is no need for interpolation if the user acquires confocal images with dx=dy=dz. We added this feature to accommodate instances where resources are insufficient to handle very large CSLM image sets. The presented interpolation methods work only for gray level images because binary images lack critical information for interpolation.

3. Three-dimensional structural parameters

From three-dimensional image sets, we can calculate two classes of parameters: textural and volumetric. Textural parameters show the microscale heterogeneity of biofilms and volumetric parameters describe the morphology of the biomass in a biofilm.

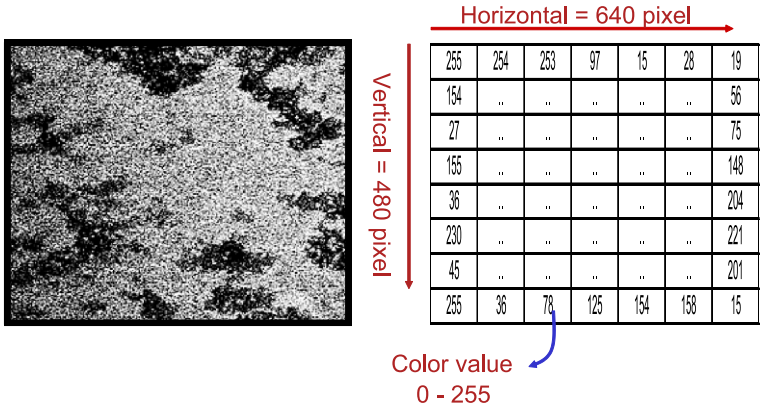

Fig. 3. A gray scale CSLM image of a sulfate-reducing biofilm acquired 50 μm above the substratum (left). Bright and dark areas show cell clusters and voids in the biofilm.

3.1. Textural parameters

Textural parameters quantify the gray scale intensity variations in biofilm images as shown in Fig. 3, where the gray scale values vary from 0 to 255. We describe three textural parameters: textural entropy, energy, and homogeneity. Textural parameters quantify biofilm structure by comparing the intensity, position, and/or orientation of the pixels. Each textural parameter measures the character of the cell cluster and interstitial spaces based on the likelihood that pixels of similar or dissimilar types will be neighbors. In our analyses, we calculated textural parameters in three dimensions according to Haralick et al. (1973) by using the gray level co-occurrence matrix (GLCM) calculated for X, Y and Z direction dependence matrices. The GLCM represents the distribution of changes in gray level values of neighboring pixels in the X, Y and Z directions. The gray level image layers are eight-bit, thus, the color values vary from 0 to 255. For simplicity, the example data set shown in Fig. 4 only varies in gray level value from 0 to 3.

The GLCM is calculated from the spatial dependence matrices. The X-spatial dependence matrix is defined and calculated as:

$$P_X = \{P_X(a,b)\} = \begin{bmatrix} P_X(0,0) & P_X(0,1) & P_X(0,2) & P_X(0,3) \\ P_X(1,0) & P_X(1,1) & P_X(1,2) & P_X(1,3) \\ P_X(2,0) & P_X(2,1) & P_X(2,2) & P_X(2,3) \\ P_X(3,0) & P_X(3,1) & P_X(3,2) & P_X(3,3) \end{bmatrix} = \begin{bmatrix} 2 & 3 & 4 & 1 \\ 3 & 2 & 1 & 2 \\ 4 & 1 & 2 & 2 \\ 1 & 2 & 2 & 4 \end{bmatrix}$$

where $P_X(a,b)$ is the number of times the gray level changes from a to b in the X direction between neighboring pixels in the image integrated over the entire image, i.e. taken from all layers. For example, $P_X(0,0)$ is 2 because ever all the layers, there are two cases where pixels that are neighbors in the X direction

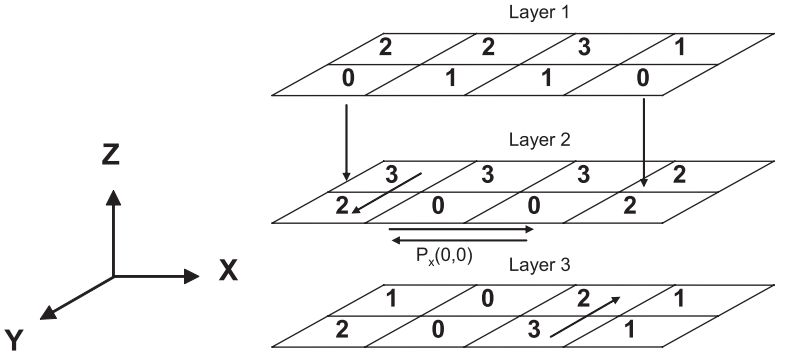

Fig. 4. Three-dimensional biofilm image with gray level values varying from 0 to 3.

(positive and negative) are both zero (see arrows in Fig. 4). Similarly, $P_X(0,1)$ is 3 as there are three locations where are 0 and 1 are neighbors, one in the left-to-right direction and two in the right-to-left direction.

The Y and Z dependence matrices are calculated in the same manner: For example, $P_Y(3,2)$ is 2 because over all the layers, there are two cases where pixels that are neighbors in the Y direction change from 3 to 2 (see arrows in Y direction in Fig. 4). Similarly, $P_Z(0,2)$ is 2 because over all the layers, there are two cases where pixels that are neighbors in the Z direction change from 0 to 2 (see arrows in Z direction in Fig. 4).

$$P_Y = \{P_Y(a,b)\} = \begin{bmatrix} P_Y(0,0) & P_Y(0,1) & P_Y(0,2) & P_Y(0,3) \\ P_Y(1,0) & P_Y(1,1) & P_Y(1,2) & P_Y(1,3) \\ P_Y(2,0) & P_Y(2,1) & P_Y(2,2) & P_Y(2,3) \\ P_Y(3,0) & P_Y(3,1) & P_Y(3,2) & P_Y(3,3) \end{bmatrix} = \begin{bmatrix} 2 & 1 & 1 & 2 \\ 1 & 2 & 2 & 1 \\ 1 & 2 & 2 & 2 \\ 2 & 1 & 2 & 0 \end{bmatrix}$$

$$P_Z = \{P_Z(a,b)\} = \begin{bmatrix} P_Z(0,0) & P_Z(0,1) & P_Z(0,2) & P_Z(0,3) \\ P_Z(1,0) & P_Z(1,1) & P_Z(1,2) & P_Z(1,3) \\ P_Z(2,0) & P_Z(2,1) & P_Z(2,2) & P_Z(2,3) \\ P_Z(3,0) & P_Z(3,1) & P_Z(3,2) & P_Z(3,3) \end{bmatrix} = \begin{bmatrix} 2 & 2 & 2 & 2 \\ 2 & 0 & 3 & 1 \\ 2 & 3 & 2 & 3 \\ 2 & 1 & 3 & 2 \end{bmatrix}$$

The spatial dependence matrix is calculated by summing the three dependence matrices.

$$P_{XYZ} = P_X + P_Y + P_Z$$

P_X | P_Y | P_Z | P_{XYZ}

2	3	4	1	2	1	1	2	2	2	2	2	6	6	7	5
3	2	1	2	1	2	2	1	2	0	3	1	6	4	6	4
4	1	2	2	1	2	2	2	2	3	2	3	7	6	6	7
1	2	2	4	2	1	2	0	2	1	3	2	5	4	7	6

(1)

The GLCM is calculated by normalizing P_{XYZ} by dividing by the sum of all the counts.

$$[\text{GLCM}] = \frac{[P_{XYZ}]}{\sum P_{XYZ}} \tag{2}$$

The sum of the elements in P_{XYZ} is 6+6+7+5+6+4+6+4+7+6+6+7+4+5+7+6=92 so the GLCM is:

$$\text{GLCM} = \frac{[P_{XYZ}]}{92} =$$

0.0652	0.0652	0.0761	0.0543
0.0652	0.0435	0.0652	0.0435
0.0761	0.0652	0.0652	0.0761
0.0543	0.0435	0.0761	0.0652

This converts the elements in the GLCM into probabilities, where $P(a,b)$ is the probability of finding a and b as the gray level values of neighboring pixels.

3.1.1. Calculation of textural parameters

From the GLCM, the following textural parameters can be calculated according to (Haralick et al., 1973):

$$\text{Energy} = \sum_{1}^{N_a}\sum_{1}^{N_b} P_N(a,b)^2 \tag{4}$$

$$\text{Textural entropy} = -\sum_{1}^{N_a}\sum_{1}^{N_b} P_N(a,b)\,\ln(P_N(a,b)) \tag{3}$$

$$\text{Homogeneity} = \sum_{1}^{N_a}\sum_{1}^{N_b} \frac{1}{1+(a-b)^2} P_N(a,b) \tag{5}$$

In this example, the computed parameters are:

$$\begin{aligned}TE = & -[(0.0652*(\ln(0.0652)) + 0.0652* \\ & \times(\ln(0.0652)) + 0.0761*(\ln(0.0761)) \\ & + 0.0543*(\ln(0.0543)) + 0.0652* \\ & \times(\ln(0.0652))\ldots]\end{aligned}$$

$$TE = 2.756$$

$$\begin{aligned}E = & 0.0652^2 + 0.0652^2 + 0.0761^2 + 0.0543^2 \\ & + 0.0652^2 + \ldots\end{aligned}$$

$$E = 0.065$$

$$\begin{aligned}H = & \frac{1}{1+(0-0)^2}*0.0652 + \frac{1}{1+(0-1)^2}*0.0652 \\ & + \frac{1}{1+(0-2)^2}*0.0761 + \frac{1}{1+(0-3)^2}*0.0543 \\ & + \frac{1}{1+(1-0)^2}*0.0652 + \ldots\end{aligned}$$

$$H = 0.504$$

3.1.2. Meaning of textural parameters

Textural entropy is a measure of randomness in the gray scale of the image. The higher the textural entropy, the more heterogeneous the image is. Fig. 5A shows an image with no structure, composed of only white pixels, or voids. The textural entropy computed for this image is zero, showing there is no gray scale variation in the pixels or heterogeneity in the image. In Fig. 5, B, C and D contain increasing numbers of clusters (spheres) and the textural entropy increases accordingly. E and F contain the same number of cell clusters (identical) but are oriented differently; they do not show significant gray level variations so the textural entropy values are similar. Increased numbers of cell clusters increase textural entropy (compare F and D) due to increased gray level variability and heterogeneity in the images.

Energy measures the regularity in patterns of pixels and it is sensitive to the orientation of the pixel clusters and the similarity of their shapes. Smaller energy values mean frequent and repeated patterns of pixel clusters, and a higher energy means a more homogeneous image structure. In Fig. 5A, the energy is one, indicating that there is no regularity in that image, but as the number of repeating clusters increases, the energy value decreases (Table 1).

Homogeneity measures the similarity of the spatially close image structures: a higher homoge-

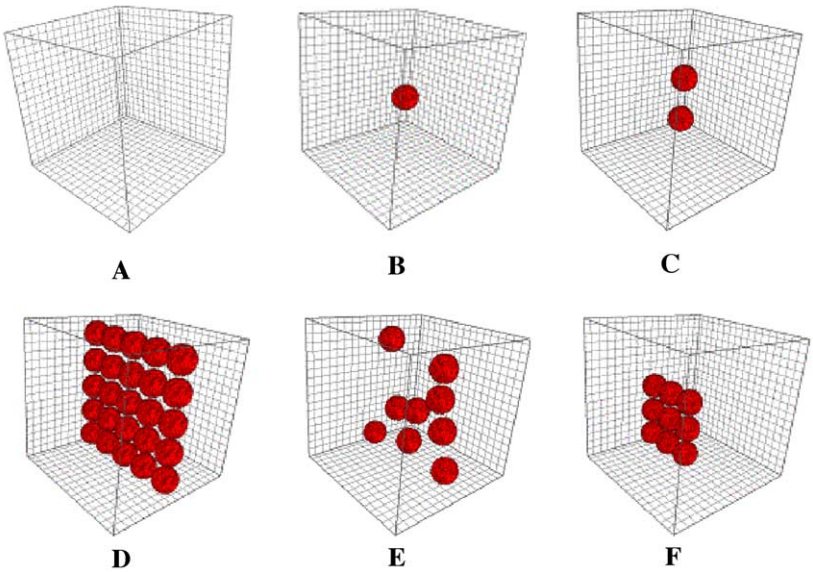

Fig. 5. Custom-generated images used to discuss meaning of textural parameters. (A) Empty image (all voids), (B) a single cell cluster made of a sphere, (C) two cell clusters, (D) many cell clusters repeating regularly, (E) nine irregularly repeating cell clusters, (F) nine cell clusters placed regularly. The images were generated using MATLAB. The textural parameters for these images are shown in Table 1.

Table 1
The textural parameters computed for the images presented in Fig. 5

Image	TE	*E*	*H*
A	0	1	1
B	0.022837	0.99416	0.998767
C	0.041726	0.988306	0.997531
D	0.336192	0.859457	0.969088
E	0.148825	0.947748	0.988684
F	0.148364	0.947984	0.988631

neity indicates a more homogeneous image structure. Homogeneity is normalized with respect to the distance between changes in texture, but it is independent of the locations of the pixel clusters in the image. In Fig. 5A, homogeneity equals one, indicating a homogeneous image; the homogeneity decreases with increasing numbers of clusters (Table 1).

Homogeneity vs. energy: The definitions of these two parameters are similar, and the meaning of these parameters requires further explanation. This may best be accomplished by comparing the images in Fig. 5. Fig. 5D contains 19 more clusters than Fig. 5C. Consequently, there is a pattern of repeating pixel clusters in the Z direction. However, the shapes of the clusters are identical. Therefore, comparing the computed parameters, it is not surprising that the energy increases more than the homogeneity does (ΔE=0.129 and ΔH=0.028). Indeed, ΔE is almost 4.5 times higher than ΔH, showing that there is significant directional variation between the structures in D of Fig. 5 and those in *E*. When we compare E and F in Fig. 5, ΔE and ΔH are very low, showing that having identical cell clusters and gray level variations does not change the values for energy and homogeneity. This shows that the decrease in homogeneity and energy is also caused by the number of cell clusters.

4. Volumetric parameters

Volumetric parameters express the morphology of biofilms and they are calculated with pixels representing biomass in the image. Each parameter quantifies a unique feature of the three-dimensional image. The volumetric parameters we describe in this paper are: average run lengths (in X, Y and Z directions), aspect ratio, average and maximum diffusion distances and fractal dimension. These parameters are calculated from a binary image, where only two gray levels are allowed. This is

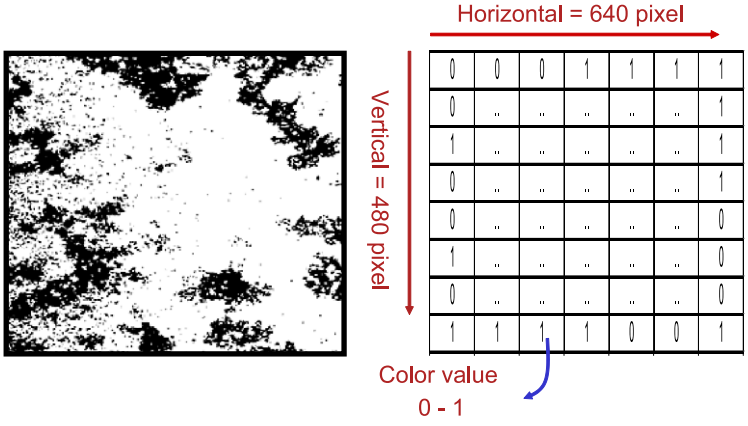

Fig. 6. Binary image of a sulfate-reducing biofilm (presented in Fig. 3) acquired 50 μm above the substratum (left). When a gray scale biofilm image is converted to a binary level image, the intensity of the gray level is represented by a one or a zero for each pixel.

accomplished by using a process known as thresholding that converts all pixel values below the threshold to zero and all pixels values above the threshold to one (Yang et al., 2001). The resulting black-and-white image has two visible components as shown in Fig. 6.

4.1. Average run lengths (X, Y and Z)

Run length measures the number of consecutive cluster pixels in a given direction, and an average run length measures the average length of consecutive cluster pixels in the measurement direction. If a biofilm has a large average X-run length and a small average Y-run length, then the biofilm appears stretched in the X direction and this may indicate the presence of streamers. It is important to consider the direction of the run length (X, Y and Z) before making conclusions since each run length is valid only for that direction (Fig. 7).

4.2. Calculation of run length

The calculation of the X run length sweeps the image (Fig. 7) in the X direction counting consecutive biomass cell pixels. Fig. 8A shows the X direction runs marked with arrows.

Starting at the top in Fig. 8A, the X direction runs are: (3+2)+(4+2)+(1+4)=16. The number of runs (total number of arrows) is 6. Thus, the average X-run length (AXRL) is 16/6=2.67. The average Y-run length (AYRL) and average Z-run length (AZRL) are calculated in the same manner.

$$\mathrm{AYRL} = [(1+2+1+1)+(1+1+2+2)+(1+1+1+2)]/12 = 1.3333$$

$$\mathrm{AZRL} = (1+1+1+1+1+2+2+2+2+3)/10 = 1.6000$$

4.3. Aspect ratio and its calculation

The aspect ratio is defined as the ratio of AXRL to AYRL. It indicates the symmetry of cluster growth in the ⟨X,Y⟩ direction.

$$\text{Aspect ratio} = \frac{\mathrm{AXRL}}{\mathrm{AYRL}} \tag{6}$$

If the aspect ratio remains constant during biofilm growth, the biofilm microcolonies grow symmetrically in the X and Y directions. If shear stress or any other action tends to deform the microcolonies in one direction, that effect is reflected in a changing aspect ratio.

4.4. Average diffusion distance.

The diffusion distance is defined as *the minimum linear distance in three dimensions from a cluster pixel to the nearest void pixel* in an image. The average diffusion distance (ADD) is the average of the

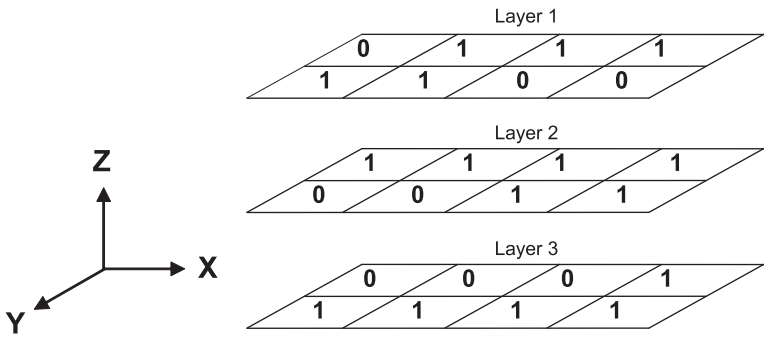

Fig. 7. 3D binary image used for average run length calculations.

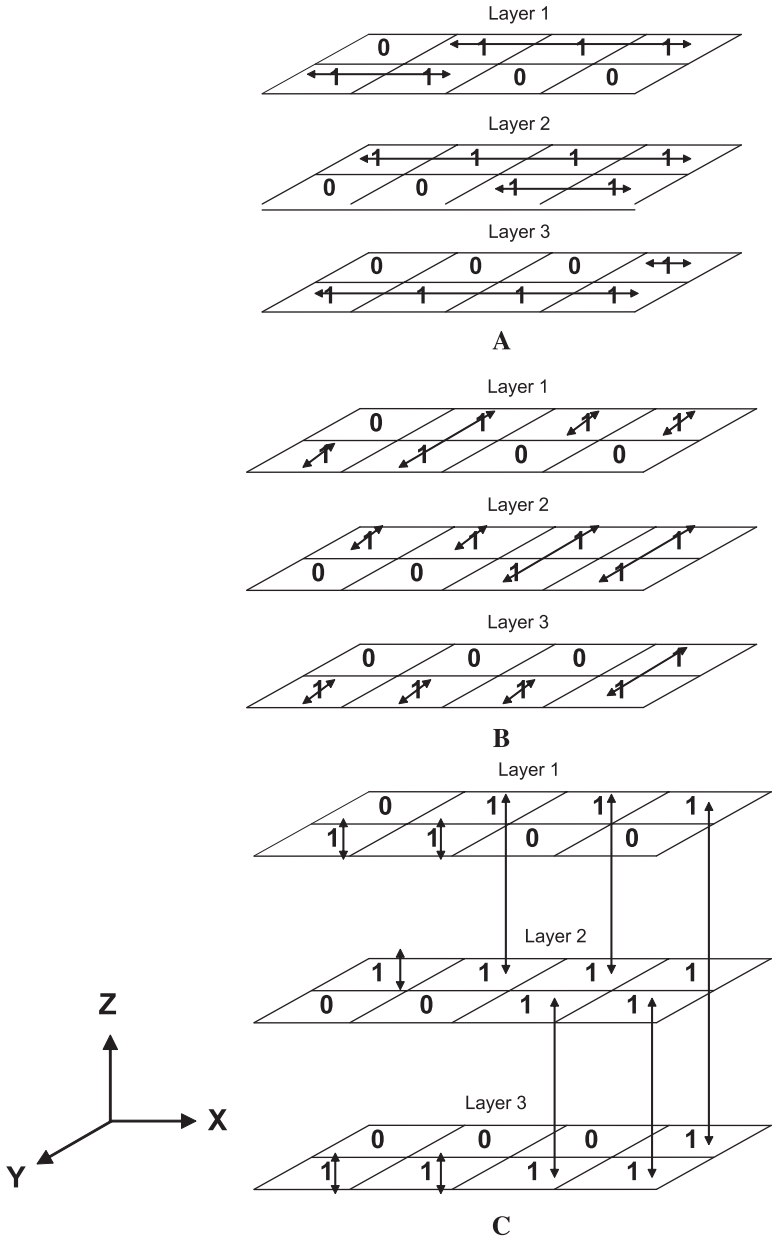

Fig. 8. (A) original 3D biofilm image with X direction runs marked, (B) original 3D biofilm image with Y direction runs marked, (C) original 3D biofilm image with Z direction runs marked.

From a process viewpoint, a larger diffusion distance indicates a larger distance over which substrate has to diffuse in the cell cluster. The maximum diffusion distance (MDD) is computed as the distance to the most "remote" pixel in the cell cluster from a void cluster.

The definition of diffusion distance refers only to the shortest distance, and it is independent of the direction. To calculate the average diffusion distance, we use the Euclidean distance mapping algorithm (Friedman et al., 1997) in three dimensions to calculate the minimum distance from each cluster cell to the nearest void pixel.

4.5. Calculation of diffusion distances

A six-layer image with cluster pixels marked as 1's (before Euclidean distance mapping) is shown below.

Layer 1

0	0	0	0	0	0	0	0
0	0	0	0	0	0	0	0
0	0	0	0	0	0	0	0
0	0	0	0	0	0	0	0
0	0	0	0	0	0	0	0
0	0	0	0	0	0	0	0
0	0	0	0	0	0	0	0
0	0	0	0	0	0	0	0

Layer 2

0	0	0	0	0	0	0	0
0	0	0	0	0	0	0	0
0	0	0	1	1	0	0	0
0	0	1	1	1	1	0	0
0	0	1	1	1	1	0	0
0	0	0	1	1	0	0	0
0	0	0	0	0	0	0	0
0	0	0	0	0	0	0	0

Layer 3

0	0	0	0	0	0	0	0
0	0	0	0	0	0	0	0
0	0	1	1	1	1	0	0
0	0	1	1	1	1	0	0
0	0	1	1	1	1	0	0
0	0	1	1	1	1	0	0
0	0	0	0	0	0	0	0
0	0	0	0	0	0	0	0

Layer 4

0	0	0	0	0	0	0	0
0	0	0	0	0	0	0	0
0	0	1	1	1	1	0	0
0	0	1	1	1	1	0	0
0	0	1	1	1	1	0	0
0	0	1	1	1	1	0	0
0	0	0	0	0	0	0	0
0	0	0	0	0	0	0	0

Layer 5

0	0	0	0	0	0	0	0
0	0	0	0	0	0	0	0
0	0	1	1	1	1	0	0
0	0	1	1	1	1	0	0
0	0	1	1	1	1	0	0
0	0	1	1	1	1	0	0
0	0	0	0	0	0	0	0
0	0	0	0	0	0	0	0

Layer 6

0	0	0	0	0	0	0	0
0	0	0	0	0	0	0	0
0	0	0	0	0	0	0	0
0	0	0	0	0	0	0	0
0	0	0	0	0	0	0	0
0	0	0	0	0	0	0	0
0	0	0	0	0	0	0	0
0	0	0	0	0	0	0	0

(1) Euclidean distance mapping is applied to produce the distance map shown below.

Layer 1

0	0	0	0	0	0	0	0
0	0	0	0	0	0	0	0
0	0	0	0	0	0	0	0
0	0	0	0	0	0	0	0
0	0	0	0	0	0	0	0
0	0	0	0	0	0	0	0
0	0	0	0	0	0	0	0
0	0	0	0	0	0	0	0

Layer 2

0	0	0	0	0	0	0	0
0	0	0	0	0	0	0	0
0	0	0	1	1	0	0	0
0	0	1	1	1	1	0	0
0	0	1	1	1	1	0	0
0	0	0	1	1	0	0	0
0	0	0	0	0	0	0	0
0	0	0	0	0	0	0	0

Layer 3

0	0	0	0	0	0	0	0
0	0	0	0	0	0	0	0
0	0	1	1	1	1	0	0
0	0	1	1.7	1.7	1	0	0
0	0	1	1.7	1.7	1	0	0
0	0	1	1	1	1	0	0
0	0	0	0	0	0	0	0
0	0	0	0	0	0	0	0

Layer 4

0	0	0	0	0	0	0	0
0	0	0	0	0	0	0	0
0	0	1	1	1	1	0	0
0	0	1	2	2	1	0	0
0	0	1	2	2	1	0	0
0	0	1	1	1	1	0	0
0	0	0	0	0	0	0	0
0	0	0	0	0	0	0	0

Layer 5

0	0	0	0	0	0	0	0
0	0	0	0	0	0	0	0
0	0	1	1	1	1	0	0
0	0	1	1	1	1	0	0
0	0	1	1	1	1	0	0
0	0	1	1	1	1	0	0
0	0	0	0	0	0	0	0
0	0	0	0	0	0	0	0

Layer 6

0	0	0	0	0	0	0	0
0	0	0	0	0	0	0	0
0	0	0	0	0	0	0	0
0	0	0	0	0	0	0	0
0	0	0	0	0	0	0	0
0	0	0	0	0	0	0	0
0	0	0	0	0	0	0	0
0	0	0	0	0	0	0	0

$$\text{Fractal dimension} = \text{FD} = 2 - \text{slope} \tag{8}$$

In layer 3, the internal points for which the nearest void pixel is located on layer two are marked with 1.7. For the upper left 1.7 pixel in layer 3 at (x_0, y_0, z_0), the nearest void is at (x_0-1, y_0-1, z_0-1). The calculation is as follows:

$$\text{Diffusion distance} = \sqrt{\Delta X^2 + \Delta Y^2 + \Delta Z^2} \tag{7}$$

For this point, the diffusion distance is $\sqrt{(-1)^2+(-1)^2+(-1)^2}=1.7$. The other internal points on layers 3 and 4 have been calculated in the same manner. The 2's on layer 4 represent a distance of 2 pixels to the nearest void.

The average diffusion distance (ADD) is the average of all the diffusion distances and the maximum diffusion distance (MDD) is the maximum distance. For this example, there are 60 cluster pixels, so adding their diffusion distances and dividing by 60 produces 66.8/60=1.1133. The maximum diffusion distance is 2.

4.6. Fractal dimension

Fractal dimension is a measure of the roughness of the boundaries of cell clusters: a higher fractal dimension indicates a more irregular cell cluster surface. In three dimensions, the fractal dimension varies from 1 to 3. A 3D fractal dimension is calculated much like a 2D fractal dimension (see Yang et al., 2000 and Beyenal et al., 2004) except that instead of sweeping out areas with increasing dilation of a circle, volume is swept out with increasing dilation of a sphere. Instead of a logarithmic relationship between the perimeter and the radius of the dilation circle, this relationship is between the surface area and the radius of the dilation sphere.

4.7. Calculation of fractal dimension

In this example, we use the image given below.

Layer 1

0	0	0	0	0	0	0	0
0	0	0	0	0	0	0	0
0	0	0	0	0	0	0	0
0	0	0	0	0	0	0	0
0	0	0	0	0	0	0	0
0	0	0	0	0	0	0	0
0	0	0	0	0	0	0	0
0	0	0	0	0	0	0	0

Layer 2

0	0	0	0	0	0	0	0
0	0	0	0	0	0	0	0
0	0	1	1	1	1	0	0
0	0	1	1	1	1	0	0
0	0	1	1	1	1	0	0
0	0	1	1	1	1	0	0
0	0	0	0	0	0	0	0
0	0	0	0	0	0	0	0

Layer 3

0	0	0	0	0	0	0	0
0	0	0	0	0	0	0	0
0	0	1	1	1	1	0	0
0	0	1	1	1	1	0	0
0	0	1	1	1	1	0	0
0	0	1	1	1	1	0	0
0	0	0	0	0	0	0	0
0	0	0	0	0	0	0	0

Layer 4

0	0	0	0	0	0	0	0
0	0	0	0	0	0	0	0
0	0	1	1	1	1	0	0
0	0	1	1	1	1	0	0
0	0	1	1	1	1	0	0
0	0	1	1	1	1	0	0
0	0	0	0	0	0	0	0
0	0	0	0	0	0	0	0

Layer 5

0	0	0	0	0	0	0	0
0	0	0	0	0	0	0	0
0	0	1	1	1	1	0	0
0	0	1	1	1	1	0	0
0	0	1	1	1	1	0	0
0	0	1	1	1	1	0	0
0	0	0	0	0	0	0	0
0	0	0	0	0	0	0	0

Layer 6

0	0	0	0	0	0	0	0
0	0	0	0	0	0	0	0
0	0	0	0	0	0	0	0
0	0	0	0	0	0	0	0
0	0	0	0	0	0	0	0
0	0	0	0	0	0	0	0
0	0	0	0	0	0	0	0
0	0	0	0	0	0	0	0

We modified the Minkowski sausage method to calculate the fractal dimension (Russ, 2002) in three dimensions because it relates naturally to image processing techniques. The modified Minkowski method measures the fractal dimension by determining the rate of change in the boundary of an object as the volume of the boundary line is increased. Highly irregular boundaries will become shorter faster as the irregularities are smoothed by a thicker boundary line. From an image processing viewpoint, dilation is used to accomplish the smoothing of the boundary line as a sphere sweeps out the boundary. We change the value of the boundary pixels to zero and all other pixels to one (see example given below), and then calculate the Euclidean distances in three dimensions to obtain the distance to the boundary for each pixel. The dilation volume is computed by varying the sphere radius and counting the number of pixels at a distance smaller than this radius value.

Plotting the natural logarithm of the dilation sphere radius against the natural logarithm of the measured volume produces a straight line, and the fractal dimension is defined as:

$$\text{Fractal dimension} = \text{FD} = 2 - \text{slope} \tag{8}$$

We calculated fractal dimension in the following steps:

(1) Show only the border pixels as ones and change the rest to zeros (see below); i.e., mark boundaries with ones.

Layer 1

0	0	0	0	0	0	0	0
0	0	0	0	0	0	0	0
0	0	0	0	0	0	0	0
0	0	0	0	0	0	0	0
0	0	0	0	0	0	0	0
0	0	0	0	0	0	0	0
0	0	0	0	0	0	0	0
0	0	0	0	0	0	0	0

Layer 2

0	0	0	0	0	0	0	0
0	0	0	0	0	0	0	0
0	0	1	1	1	1	0	0
0	0	1	1	1	1	0	0
0	0	1	1	1	1	0	0
0	0	1	1	1	1	0	0
0	0	0	0	0	0	0	0
0	0	0	0	0	0	0	0

Layer 3

0	0	0	0	0	0	0	0
0	0	0	0	0	0	0	0
0	0	1	1	1	1	0	0
0	0	1	0	0	1	0	0
0	0	1	0	0	1	0	0
0	0	1	1	1	1	0	0
0	0	0	0	0	0	0	0
0	0	0	0	0	0	0	0

Layer 4

0	0	0	0	0	0	0	0
0	0	0	0	0	0	0	0
0	0	1	1	1	1	0	0
0	0	1	0	0	1	0	0
0	0	1	0	0	1	0	0
0	0	1	1	1	1	0	0
0	0	0	0	0	0	0	0
0	0	0	0	0	0	0	0

Layer 5

0	0	0	0	0	0	0	0
0	0	0	0	0	0	0	0
0	0	1	1	1	1	0	0
0	0	1	1	1	1	0	0
0	0	1	1	1	1	0	0
0	0	1	1	1	1	0	0
0	0	0	0	0	0	0	0
0	0	0	0	0	0	0	0

Layer 6

0	0	0	0	0	0	0	0
0	0	0	0	0	0	0	0
0	0	0	0	0	0	0	0
0	0	0	0	0	0	0	0
0	0	0	0	0	0	0	0
0	0	0	0	0	0	0	0
0	0	0	0	0	0	0	0
0	0	0	0	0	0	0	0

(2) Invert the pixels: change the ones to zeros and the zeros to ones (see below).

Layer 1

1	1	1	1	1	1	1	1
1	1	1	1	1	1	1	1
1	1	1	1	1	1	1	1
1	1	1	1	1	1	1	1
1	1	1	1	1	1	1	1
1	1	1	1	1	1	1	1
1	1	1	1	1	1	1	1
1	1	1	1	1	1	1	1

Layer 2

1	1	1	1	1	1	1	1
1	1	1	1	1	1	1	1
1	1	0	0	0	0	1	1
1	1	0	0	0	0	1	1
1	1	0	0	0	0	1	1
1	1	0	0	0	0	1	1
1	1	1	1	1	1	1	1
1	1	1	1	1	1	1	1

Layer 3

1	1	1	1	1	1	1	1
1	1	1	1	1	1	1	1
1	1	0	0	0	0	1	1
1	1	0	1	1	0	1	1
1	1	0	1	1	0	1	1
1	1	0	0	0	0	1	1
1	1	1	1	1	1	1	1
1	1	1	1	1	1	1	1

Layer 4

1	1	1	1	1	1	1	1
1	1	1	1	1	1	1	1
1	1	0	0	0	0	1	1
1	1	0	1	1	0	1	1
1	1	0	1	1	0	1	1
1	1	0	0	0	0	1	1
1	1	1	1	1	1	1	1
1	1	1	1	1	1	1	1

Layer 5

1	1	1	1	1	1	1	1
1	1	1	1	1	1	1	1
1	1	0	0	0	0	1	1
1	1	0	0	0	0	1	1
1	1	0	0	0	0	1	1
1	1	0	0	0	0	1	1
1	1	1	1	1	1	1	1
1	1	1	1	1	1	1	1

Layer 6

1	1	1	1	1	1	1	1
1	1	1	1	1	1	1	1
1	1	1	1	1	1	1	1
1	1	1	1	1	1	1	1	1
1	1	1	1	1	1	1	1
1	1	1	1	1	1	1	1
1	1	1	1	1	1	1	1
1	1	1	1	1	1	1	1

.

Steps 1 and 2 mark the boundaries of the cell clusters with zeros. Note that the boundary is defined for any direction.

(3) Use Euclidian distance mapping in three dimensions (see example given for diffusion distance) to calculate the distance to cluster void (zero) pixels for each boundary pixel (Friedman et al., 1997).

Layer 1

3	2.4	2.2	2.2	2.2	2.2	2.4	3
2.4	1.7	1.4	1.4	1.4	1.4	1.7	2.4
2.2	1.4	1	1	1	1	1.4	2.2
2.2	1.4	1	1	1	1	1.4	2.2
2.2	1.4	1	1	1	1	1.4	2.2
2.2	1.4	1	1	1	1	1.4	2.2
2.4	1.7	1.4	1.4	1.4	1.4	1.7	2.4
3	2.4	2.2	2.2	2.2	2.2	2.4	3

Layer 2

2.8	2.2	2	2	2	2	2.2	2.8
2.2	1.4	1	1	1	1	1.4	2.2
2	1	0	0	0	0	1	2
2	1	0	0	0	0	1	2
2	1	0	0	0	0	1	2
2	1	0	0	0	0	1	2
2.2	1.4	1	1	1	1	1.4	2.2
2.8	2.2	2	2	2	2	2.2	2.8

Layer 3

2.8	2.2	2	2	2	2	2.2	2.8
2.2	1.4	1	1	1	1	1.4	2.2
2	1	0	0	0	0	1	2
2	1	0	1	1	0	1	2
2	1	0	1	1	0	1	2
2	1	0	0	0	0	1	2
2.2	1.4	1	1	1	1	1.4	2.2
2.8	2.2	2	2	2	2	2.2	2.8

Layer 4

2.8	2.2	2	2	2	2	2.2	2.8
2.2	1.4	1	1	1	1	1.4	2.2
2	1	0	0	0	0	1	2
2	1	0	1	1	0	1	2
2	1	0	1	1	0	1	2
2	1	0	0	0	0	1	2
2.2	1.4	1	1	1	1	1.4	2.2
2.8	2.2	2	2	2	2	2.2	2.8

Layer 5

2.8	2.2	2	2	2	2	2.2	2.8
2.2	1.4	1	1	1	1	1.4	2.2
2	1	0	0	0	0	1	2
2	1	0	0	0	0	1	2
2	1	0	0	0	0	1	2
2	1	0	0	0	0	1	2
2.2	1.4	1	1	1	1	1.4	2.2
2.8	2.2	2	2	2	2	2.2	2.8

Layer 6

3	2.4	2.2	2.2	2.2	2.2	2.4	3
2.4	1.7	1.4	1.4	1.4	1.4	1.7	2.4
2.2	1.4	1	1	1	1	1.4	2.2
2.2	1.4	1	1	1	1	1.4	2.2
2.2	1.4	1	1	1	1	1.4	2.2
2.2	1.4	1	1	1	1	1.4	2.2
2.4	1.7	1.4	1.4	1.4	1.4	1.7	2.4
3	2.4	2.2	2.2	2.2	2.2	2.4	3

The above matrix shows Euclidian distance mapping.

(4) For each dilation, count the number of pixels with distances less than or equal to the sphere radius. The sphere radius starts at 1 and increases by 1. In this example, we will start from 1 and increase by 0.5 since our image matrix is very small compared to real biofilm image matrices. For example, if the radius value is 1.5, we simply count the number of pixels less than or equal to 1.5. We sum one layer at a time, so 32+36+36+36+36+32=208. Then we calculate the volume/radius ratio, which is 208/1.5=138.66. This process is repeated for increasing radius values. When the natural logarithm of the sphere radius vs. the natural logarithm of the volume/radius ratio is plotted, it produces a straight line, as shown in Fig. 9.

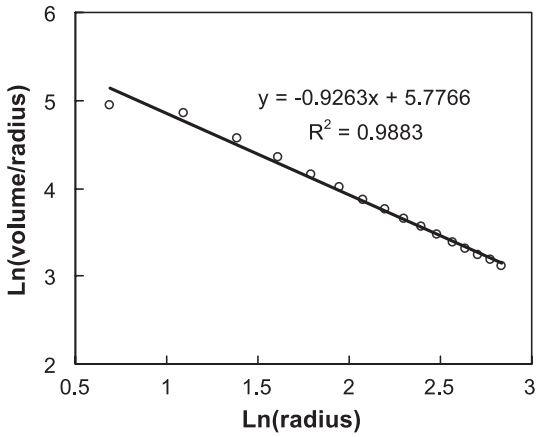

Fig. 9. Ln(volume/radius) vs. Ln(radius).

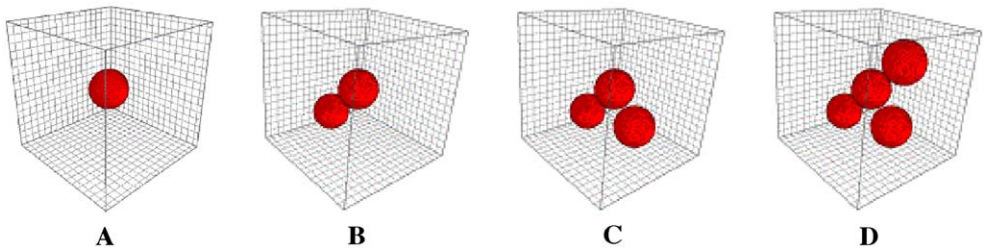

Fig. 10. (A) A single cell cluster, (B) two cell clusters, (C) three cell clusters and (D) four cell clusters.

For our example, the slope of the line is −0.93. Thus, the fractal dimension is 2−(−0.93)=2.93. FD is 1 for a line (in 3D) and 2 for a sphere (in 3D). For an extremely rough boundary structure, the fractal dimension approaches a limit of 3.

4.8. The meaning of volumetric parameters

To expose the meaning of the volumetric parameters as for the textural parameters, we generated a set of images (Fig. 10) with spherical cell clusters as shown in Fig. 10A.

As seen in Table 2, the ADD, MDD, AXRL, AYRL and AZRL are the same for each image. This is expected since identical cell clusters should have identical values for these parameters. Although all spheres are identical, slight variations in fractal dimension values are caused by interactions between the borders of the spheres.

5. Results and discussion

5.1. ISA3D software to calculate the parameters automatically

The goal of this research was to describe each parameter and demonstrate its calculation step by step so that someone could perform the calculations using a hand calculator. For biofilm images, it is impossible to perform these calculations manually, so we integrated the algorithms presented here in software called Image Structure Analyzer in 3 Dimensions (ISA3D). ISA3D was written using Matlab 7. In addition to the parameters presented in this paper, ISA3D can calculate parameters described by COMSTAT and Xavier et al.'s software (Beyenal et al., 2004; Heydorn et al., 2000; Xavier et al., 2003; Yang et al., 2000). These parameters are: biovolume, volume to surface area ratio, porosity, surface area between biomass and voids, mean thickness, maximum thickness, and roughness coefficient. In addition, we combined our previous software, ISA (Yang et al., 2000) with ISA3D, so the user can analyze textural entropy, homogeneity, energy, areal porosity, average horizontal and vertical run lengths, diffusion distance, and fractal dimension in two-dimensional image layers and quantify their distributions with biofilm thickness. The software is available from the authors upon request. Detailed information about the software will be available on the web (www.erc.montana.edu) prior to the publication of the paper.

5.2. Volumetric parameters calculated for known shapes

Before using the ISA3D software, we tested all the parameters using known shapes such as custom cubes, spheres and lines of different sizes and we calculated all parameters analytically and using ISA3D. For all tests, the results from analytical calculations and the software were the same. In addition, we generated sphere images (as in Fig. 5B) with different radii and calculated volumetric parameters to test the relationships between the parameters and to discover their physical meaning. Some selected parameters and their correlations are presented in Fig. 11. As expected, MDD corresponds to the sphere radius. For a sphere, AXRL, AYRL and AZRL must be equal because the numbers of runs in the X, Y and Z directions are the same. In another words, the aspect ratio must be equal to 1.

Table 2
The computed average (ADD) and maximum (MDD) diffusion distances, average run lengths (AXRL, AYRL and AZRL) and fractal dimensions (FD) for the images given in Fig. 10

Image	ADD (μm)	MDD (μm)	AXRL (μm)	AYRL (μm)	AZRL (μm)	FD
A	4.03	15	20.08	20.08	20.08	2.11
B	4.03	15	20.08	20.08	20.08	2.03
C	4.03	15	20.08	20.08	20.08	1.99
D	4.03	15	20.08	20.08	20.08	1.98

Although we extensively tested ISA3D using custom-generated shapes, as a further test we used bead images acquired using CSLM in which the beads had a 15-μm diameter (k=1.46). Using ISA3D, we calculated the MDD (which should be equal to the diameter of the beads) as 16.7 μm, which is close to the actual value. We believe the slight difference is due to noise in the CSLM image and the magnification used. Our experience shows that the higher magnification produced the closer value to the actual bead diameter. The aspect ratio was calculated as 1.06, which is close to the correct value of 1. This test shows that ISA3D can calculate volumetric parameter values with reasonable accuracy.

5.3. Comparing available software and ISA3D

We compare currently available software in Table 3, which shows that ISA3D covers most of the parameters other software can calculate and introduces new parameters in three dimensions. Currently there are three other software packages available: COMSTAT, Xavier et al. (2003) software and ISA (Heydorn et al., 2000; Xavier et al., 2003; Yang et al., 2000). Two-dimensional CSLM image layers can be analyzed using ISA and many of the parameters which COMSTAT and Xavier et al. (2003) software calculates can be calculated (see Table 4). COMSTAT can calculate all of the parameters that Xavier et al. (2003) software can calculate. However, Xavier's software can threshold the images automatically while COMSTAT requires manual thresholding. ISA3D has automatic thresholding. We believe the introduction of new parameters as described in this paper will be useful in biofilm research.

5.4. Textural and volumetric parameters computed from real biofilm images

Two biofilm images are compared in Fig. 12. The biofilm was composed of sulfate-reducing bacteria *Desulfovibrio desulfuricans* G20, which was used to

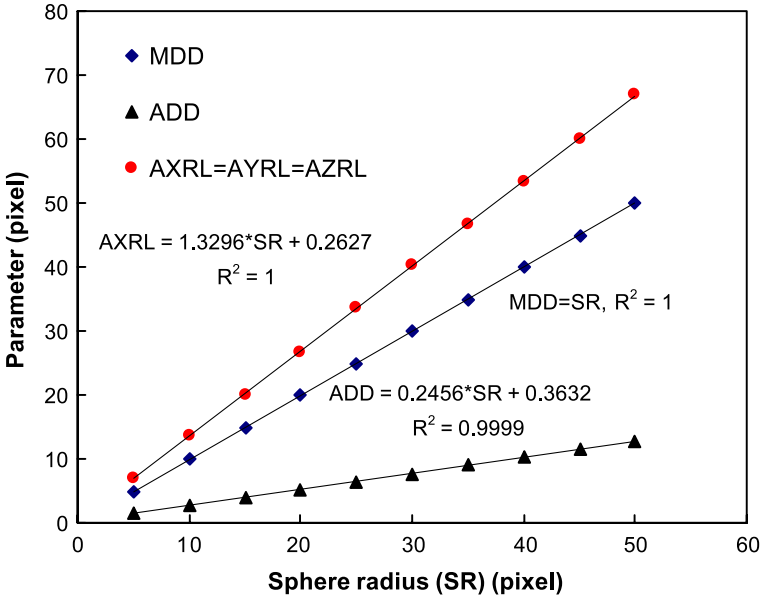

Fig. 11. The variation of ADD, MDD, AXRL, AYRL and AZRL for spheres with different radii.

Table 3
Comparing currently available software and ISA3D

No.	Parameter	ISA3D	COMSTAT	Xavier et al. (2003) software	ISA
1	Biovolume	+	+	+	+[a]
2	Volume to surface area ratio (or surface to volume ratio)	+	+	–	+[a]
3	Area occupied by each layer	+	+	–	+
4	Porosity	+	+[a]	+[a]	+[a]
5	Average diffusion distance	+	Only 2D distribution	–	Only 2D distribution
6	Average maximum diffusion distance	+	Only 2D distribution	–	Only 2D distribution
7	Surface area	+	+	+	–
8	Fractal dimension	+	Only 2D distribution	–	Only 2D distribution
9	Average X-run length	+	–	–	Only 2D distribution
10	Average Y-run length	+	–	–	Only 2D distribution
11	Average Z-run length	+	–	–	–
12	Aspect ratio in 3D	+	–	–	–
13	Textural entropy	+	–	–	Only 2D distribution
14	Energy	+	–	–	Only 2D distribution
15	Homogeneity	+	–	–	Only 2D distribution
16	Mean thickness	+	+	–	–
17	Maximum thickness	+ additionally can calculate % maximums	+	–	–
18	Roughness coefficient	+	+	–	–
19	Identification and area distribution of microcolonies at the substratum	–	+	–	Only area coverage at substratum[a]
20	Volume of the microcolonies identified at the substratum	+	+	–	+[a]
	Options				
1	Automatic thresholding	+	–	+	+
2	Interpolation	+	–	–	–
3	Automatic image reversing	+	–	–	+

[a] The given parameter can be indirectly calculated by the user using the parameters provided by the software.

reduce dissolved uranium. To acquire the images and to visualize the biofilms, we used a Leica TCS-NT confocal scanning laser microscope with 488-nm excitation and a 510-nm emission filter. The voxel width, height and depth were 1.5 μm. Textural and volumetric parameters described in this paper and additional parameters calculated using ISA3D by following the descriptions given by Heydorn et al. (2000) computed from these images are in Table 4.

The biofilm in Fig. 12A has more structures, i.e. more cell clusters, than that in Fig. 12B. However, Fig. 12A has approximately same-sized cell clusters while Fig. 12B has cluster sizes widely ranged. Visually we can expect that Fig. 12B should have a larger TE than 12B due to higher gray level variations in Fig. 12B. Since homogeneity is higher for Fig. 12A, it has fewer spatially repeating gray level variations than Fig. 12B. However, both images have very low energy showing directionally repeating variations.

Visually, we expect that Fig. 12B should have higher cell sizes, i.e. higher ADD and MDD. As expected, ADD is slightly higher and MDD is 1.8 times higher (since it has a large cluster) for Fig. 12B. The aspect ratio is close to 1 for both images, showing the circularity of the cell clusters. The results in Table 4 correspond to our expectation, showing that the parameters reflect our visual observations.

5.5. Are the biofilms in Fig. 12A and B same?

Table 4 also includes additional parameters calculated using ISA3D. We will use all of the parameters

Table 4
Textural and volumetric parameters computed from the images in Fig. 12

Image	Textural parameters			Volumetric parameters						
	TE	*E*	*H*	ADD (μm)	MDD (μm)	FD	AXRL (μm)	AYRL (μm)	AZRL (μm)	AR
A	7.31	0.0015	0.2941	2.36	14.65	2.91	12.31	11.51	4.36	1.07
B	8.78	0.00051	0.2224	2.59	22.65	2.84	11.82	11.09	4.28	1.07

Image	Additional parameters						
	Biovolume (μm^3)	Biomass volume to surface area ratio (μm)	Porosity	Surface area between biomass and void (μm^2)	Mean thickness (μm)	Maximum biofilm thickness (μm)	Roughness coefficient
A	12×10^6	1.93	0.57	6.3×10^6	46.20	52.73	0.162
B	86×10^6	2.05	0.68	4.2×10^6	39.93	46.88	0.165

Additional parameters calculated using ISA3D by following the descriptions given by Heydorn et al. (2000).

to test whether the biofilms in Fig. 12A and B are the same. If we use previously described parameters such as mean thickness, we can conclude that these biofilms are different. However, when we use the roughness coefficient as criteria, we concluded that these biofilms are the same. The roughness coefficient indicates the variability in the biofilm thickness (Heydorn et al., 2000) but does not describe the variability in the surface of the cell clusters. Fractal dimension describes variability of the cell cluster surface in three dimensions. When we compare the differences in fractal dimension (2.91–2.84=0.13) and roughness coefficient (0.162–0.165=−0.03), we find that the differences in fractal dimension are more indicative of surface variability. This shows that fractal dimension in three dimensions is more sensitive to the changes in biofilm structure than the previously described parameters. However, we still do not know whether the difference in fractal dimensions is sufficient to claim that these biofilms are different. In general, it is impossible to objectively decide when two biofilms are different. This distinction must be based on an arbitrary definition of a significant difference, e.g. if the difference between measured parameters is more than 10%, then the biofilms are different.

When we compare AXRL, AYRL, AZRL and ADD for the biofilms in Fig. 12, we find that their values are close to each other, showing that the average sizes of the cell clusters are approximately the same. We can conclude that these biofilms are composed of similarly sized cell clusters. We cannot draw the same conclusion using the mean thickness or roughness coefficient. This also shows that three-dimensional parameters are superior and more descriptive in quantifying biofilm morphology. It is also worthwhile to note that the maximum diffusion distance for the biofilm in Fig. 12B is significantly longer, showing the existence of a large cluster in this image.

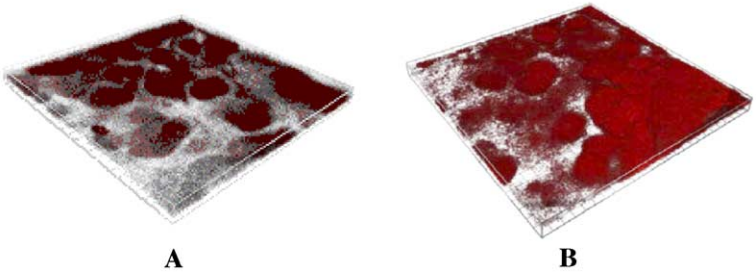

Fig. 12. Two biofilm images are analyzed verbally and digitally in Table 4.

6. Conclusions

1. We described the calculation of average and maximum diffusion distances, fractal dimension, average run lengths (in X, Y and Z directions), aspect ratio, textural entropy, energy and homogeneity from 3D images acquired by CSLM.
2. We introduced average X, Y and Z directions run lengths, fractal dimension, diffusion distances and textural entropy, energy and homogeneity as new parameters for *three-dimensional* biofilm structure quantification.
3. We illustrated the calculation of each parameter with simple examples so that the reader can perform the calculations manually and understand its meaning better.
4. The described algorithms are integrated into software called ISA3D and we demonstrated the application of ISA3D to confocal images.
5. The three-dimensional parameters described in this paper are superior and more descriptive in quantifying the biofilm morphology than previously described one-dimensional parameters.

Nomenclature

a	Integer number
ADD	Average diffusion distance
AR	Aspect ratio
AXRL	Average X-run length
AYRL	Average Y-run length
AZRL	Average Z-run length
b	Integer number
dx	The size of a pixel in the X direction
dy	The size of a pixel in the Y direction
dz	Distance between interpolated image layers
dz'	The distance between CSLM images before interpolation
E	Energy
FD	Fractal dimension
H	Homogeneity
k	Thickness of a single-layer CSLM image (=dx=dy=dz)
MDD	Maximum diffusion distance
N	The number of thickness measurements
R	Linear regression coefficient
SR	Sphere radius
TE	Textural entropy
x,y	Any x, y point in a 2D layer
x, y, z	Any x, y, z point in a 3D image
x_0, y_0	A specific x, y point in a 2D layer
x_0, y_0, z_0	A specific x, y, z point in a 3D image

Acknowledgements

Conrad Donavan was supported by the Montana State University Undergraduate Scholarship Program. The authors thank Sarah Golden for providing bead images.

References

Battin, T.J., Kaplan, L.A., Newbold, J.D., Cheng, X.H., Hansen, C., 2003. Effects of current velocity on the nascent architecture of stream microbial biofilms. Applied and Environmental Microbiology 69, 5443–5452.

Beyenal, H., Lewandowski, Z., Harkin, G., 2004. Quantifying biofilm structure: facts and fiction. Biofouling 20, 1–23.

Christensen, B.B., Haagensen, J.A.J., Heydorn, A., Molin, S., 2002. Metabolic commensalism and competition in a two-species microbial consortium. Applied and Environmental Microbiology 68, 2495–2502.

Friedman, J.H., Bentley, J.L., Raphael, R.A., 1997. ACM Transactions on Mathematical Software 3, 209–226.

Haralick, R.M., Shanmuga, K., Dinstein, I., 1973. Textural features for image classification. IEEE Transactions on Systems, Man, and Cybernetics SMC3, 610–621.

Hentzer, M., Teitzel, G.M., Balzer, G.J., Heydorn, A., Molin, S., Givskov, M., Parsek, M.R., 2001. Alginate overproduction affects *Pseudomonas aeruginosa* biofilm structure and function. Journal of Bacteriology 183, 5395–5401.

Heydorn, A., Nielsen, A.T., Hentzer, M., Sternberg, C., Givskov, M., Ersboll, B.K., Molin, S., 2000. Quantification of biofilm structures by the novel computer program COMSTAT. Microbiology (UK) 146, 2395–2407.

Heydorn, A., Ersboll, B., Kato, J., Hentzer, M., Parsek, M.R., Tolker-Nielsen, T., Givskov, M., Molin, S., 2002. Statistical analysis of *Pseudomonas aeruginosa* biofilm development: Impact of mutations in genes involved in twitching motility, cell-to-cell signaling, and stationary-phase sigma factor expression. Applied and Environmental Microbiology 68, 2008–2017.

Hinsa, S.M., Espinosa-Urgel, M., Ramos, J.L., O'Toole, G.A., 2003. Transition from reversible to irreversible attachment during biofilm formation by *Pseudomonas fluorescens* WCS365 requires an ABC transporter and a large secreted protein. Molecular Microbiology 49, 905–918.

Kierek, K., Watnick, P.I., 2003. Environmental determinants of *Vibrio cholerae* biofilm development. Applied and Environmental Microbiology 69, 5079–5088.

Kuehn, M., Hausner, M., Bungartz, H.J., Wagner, M., Wilderer, P.A., Wuertz, S., 1998. Automated confocal laser scanning

microscopy and semiautomated image processing for analysis of biofilms. Applied and Environmental Microbiology 64, 4115–4127.

Mah, T.F., Pitts, B., Pellock, B., Walker, G.C., Stewart, P.S., O'Toole, G.A., 2003. A genetic basis for *Pseudomonas aeruginosa* biofilm antibiotic resistance. Nature 426, 306–310.

Martiny, A.C., Jorgensen, T.M., Albrechtsen, H.J., Arvin, E., Molin, S., 2003. Long-term succession of structure and diversity of a biofilm formed in a model drinking water distribution system. Applied and Environmental Microbiology 69, 6899–6907.

Russ, J., 2002. The Image Processing Handbook. CRC Press, Boca Raton.

Xavier, J.B., Schnell, A., Wuertz, S., Palmer, R., White, D.C., Almeida, J.S., 2001. Objective threshold selection procedure (OTS) for segmentation of scanning laser confocal microscope images. Journal of Microbiological Methods 47, 169–180.

Xavier, J.B., White, D.C., Almeida, J.S., 2003. Automated biofilm morphology quantification from confocal laser scanning microscopy imaging. Water Science and Technology 47, 31–37.

Yang, X.M., Beyenal, H., Harkin, G., Lewandowski, Z., 2000. Quantifying biofilm structure using image analysis. Journal of Microbiological Methods 39, 109–119.

Yang, X.M., Beyenal, H., Harkin, G., Lewandowski, Z., 2001. Evaluation of biofilm image thresholding methods. Water Research 35, 1149–1158.